SUPPLEMENTAL FIGURES

Enhanced glycolytic metabolism supports transmigration of brain-infiltrating macrophages in multiple sclerosis

Deepak Kumar Kaushik[1], Anindita Bhattacharya[1], Reza Mirzaei[1], Khalil S. Rawji[1], Younghee Ahn[2], Jong M. Rho[2, 3], V. Wee Yong[1,*]

[1]Hotchkiss Brain Institute and [2]Alberta Children Hospital Research Institute,
and the Department of Clinical Neurosciences,
[3]Department of Pediatrics, Clinical Neurosciences and Physiology & Pharmacology
University of Calgary,
Calgary, Canada

*Address correspondence to:

V. Wee Yong, PhD

Professor, University of Calgary

3330 Hospital Drive

Calgary, Alberta T2N 4N1

Canada

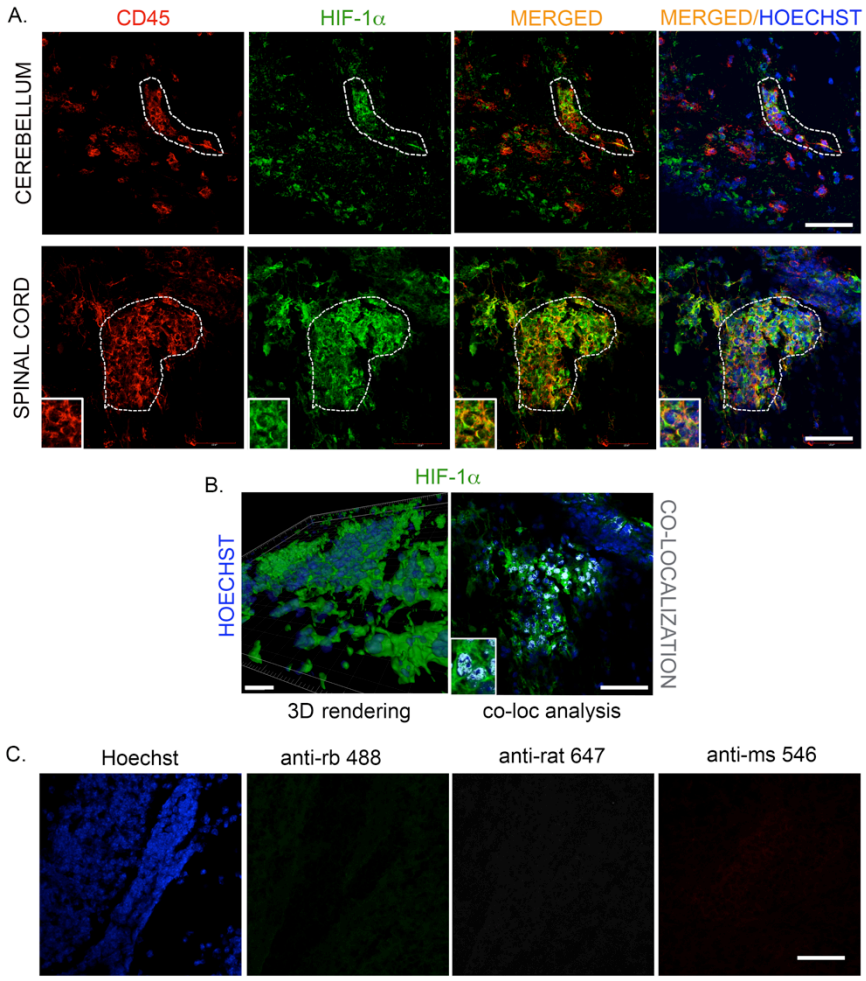

Figure S1: Leukocytes in the perivascular cuffs express HIF-1α, a critical regulator of aerobic glycolysis. A) Expression of HIF-1α (green) in CD45+ (red) cells in cerebellar and spinal cord cuffs in D16 EAE mice. Scale bar – 50 μm. **B)** 3D reconstruction of HIF-1α and Hoechst+ (blue) nuclei showing both the cytoplasmic and nuclear expression of HIF-1α within the cells in a spinal cord cuff. Scale bar – 20 μm; another panel depicts co-localization of HIF-1α with nuclei to emphasize on its role as a transcription factor. Representative images of 6 perivascular cuffs from 3 EAE afflicted mice. **C)** 'Secondary antibody only' controls showing perivascular cuffs in EAE cerebellum stained for Hoechst, anti-rabbit 488 (anti-rb 488), anti-rat 647, and anti-mouse 546 (anti-ms 546). Scale bar – 50 μm.

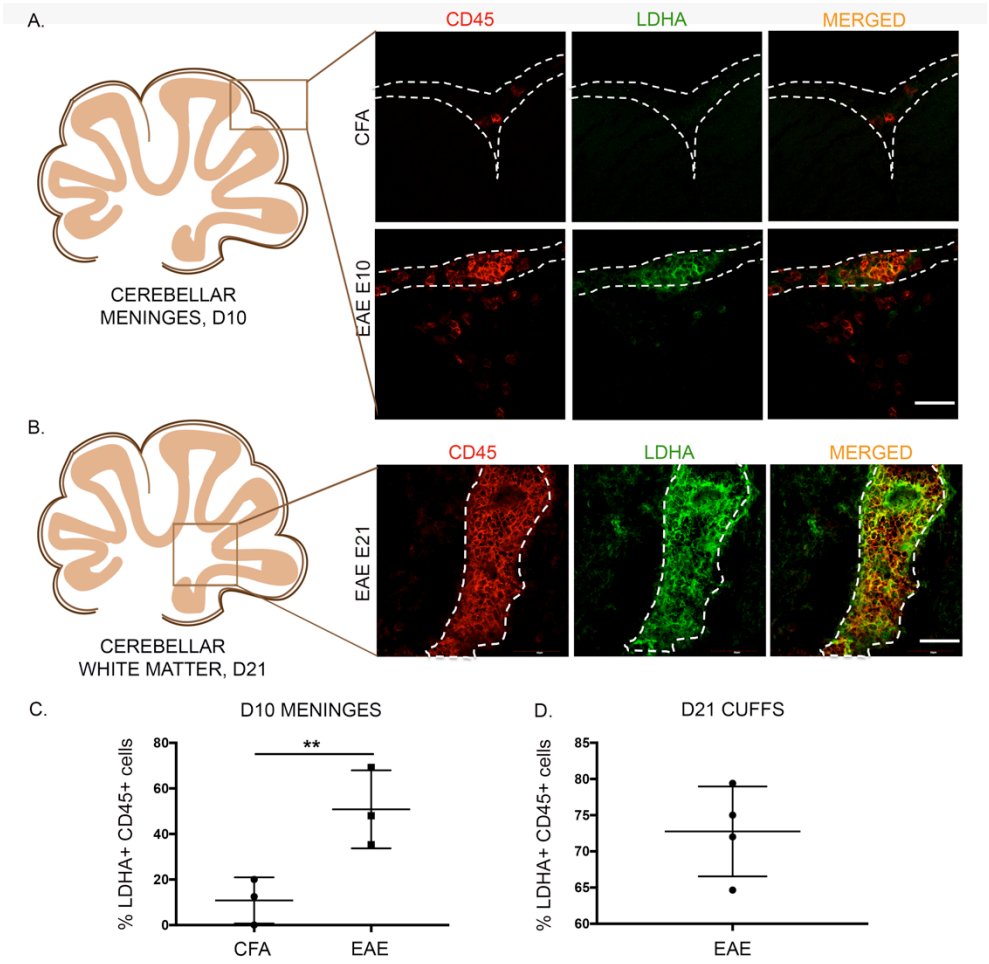

Figure S2. LDHA is expressed during the onset of EAE symptoms within the meningeal leukocytes and also at a later time-point in perivascular cuffs. A) LDHA expressing CD45+ cells within the meningeal barriers are witnessed as early as D10 during the disease course of EAE as compared to the complete Freund's adjuvant (CFA) control. **B)** Representative images of post-peak (D21) perivascular cuffs showing prominent expression of LDHA within leukocytes. n=3 mice per group. Scale bar – 50 µm. **C)** Percentage of LDHA+ leukocytes in meninges of 3 D10 EAE mice over CFA control. **D)** Graph showing percentage of LDHA+ leukocytes in D21 perivascular cuffs representative of 4 cuffs over 3 mice. Graphs are represented as mean ± SD; groups were compared using two-tailed Student's t-test.**p<0.01.

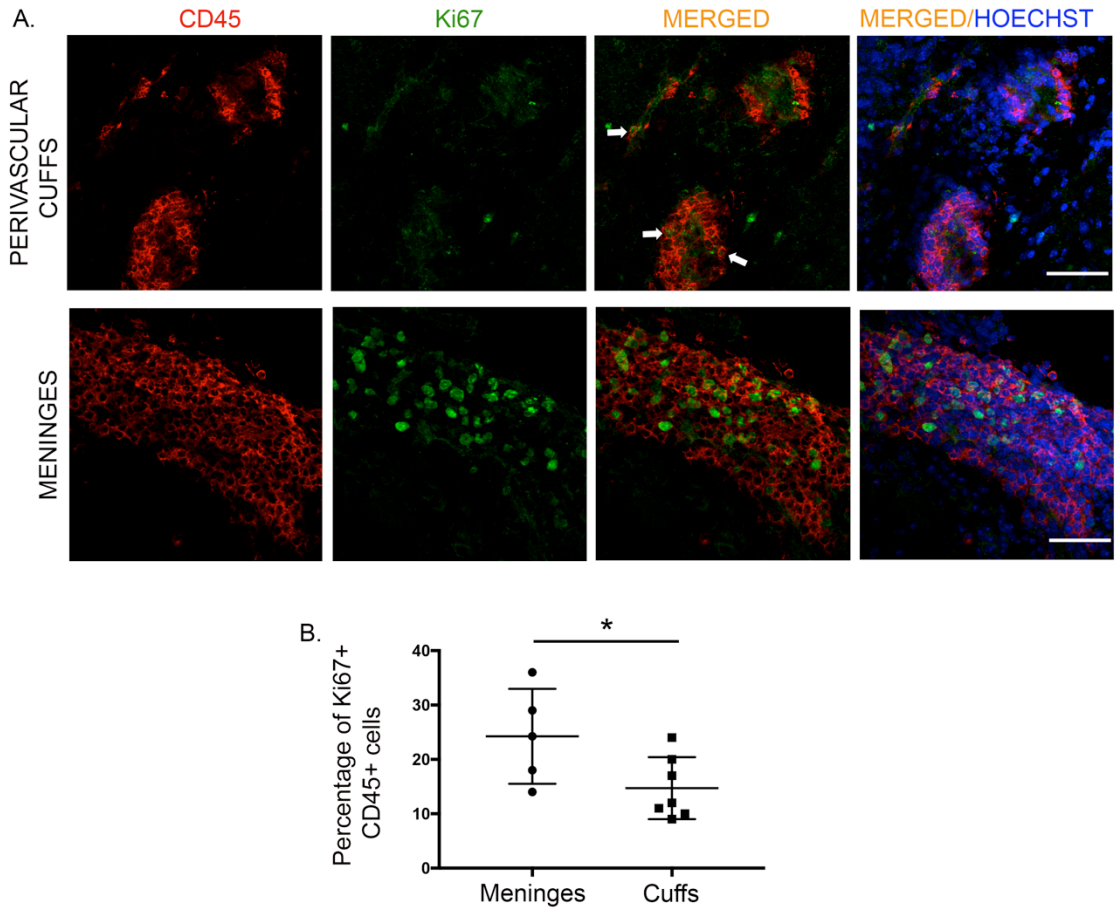

Figure S3. Fewer leukocytes proliferate within the perivascular cuffs compared to those in meninges. A) Representative images of perivascular cuffs (upper panel) and meningeal barrier (lower panel) in D16 EAE showing Ki67+ (proliferative) CD45+ leukocytes. **B)** Graph showing significantly reduced number of Ki67+ leukocytes within the perivascular cuff as compared to meninges in EAE cerebellum (n=5/6). Scale bar – 50 μm; n=3; groups were compared with two-tailed Student's t-test; *$p<0.05$.

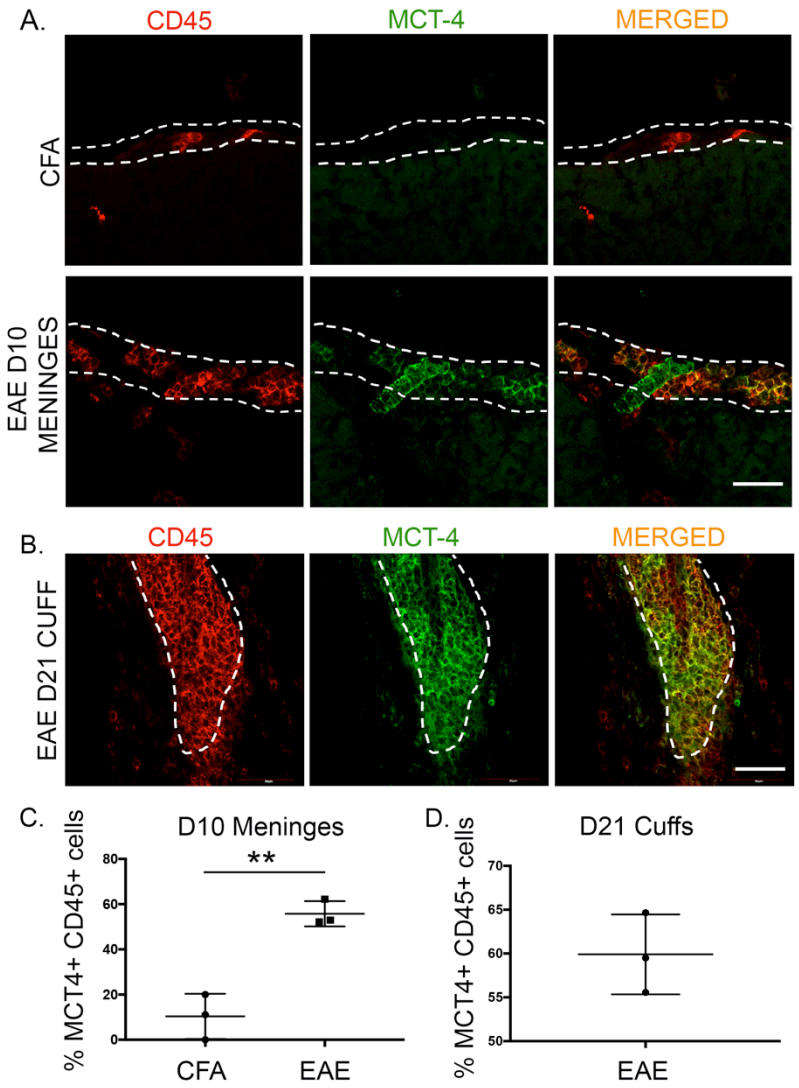

Figure S4. Expression of MCT-4 in D10 meninges and D21 perivascular cuffs. A) Similar to LDHA, we found that MCT-4 expressing leukocytes were prominent as early as D10 EAE in meninges (lower panel) as compared to the CFA-injected mice (upper panel). **B)** MCT-4 expression was seen in CD45+ cells even in perivascular cuffs during later time course (D21 EAE). **C)** Graph showing the percentage of MCT4+ leukocytes in meninges of D10 EAE mice as compared to CFA control. **D)** Graph showing percentage of MCT4+ leukocytes in perivascular cuffs of D21 EAE mice; n=3 mice per group; groups were compared using two-tailed Student's t-test. **p<0.01. scale bar – 50 μm.

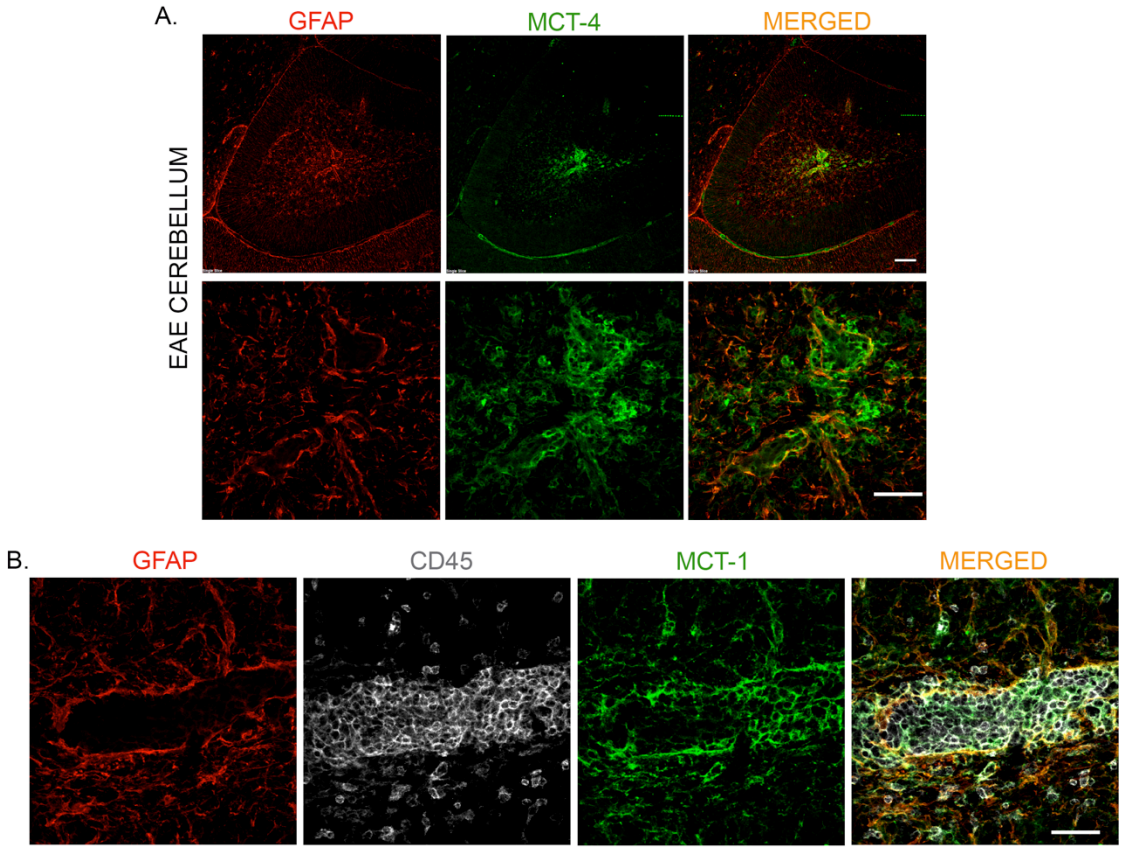

Figure S5. Expression of MCT-1 and MCT-4 in GFAP+ astrocytes in D16 EAE. A) MCT-4 expression (green) in GFAP+ astrocytes (red) that abutted the perivascular cuffs in D16 EAE cerebellum as seen in low magnification (upper panel; scale bar – 100 μm) as well as the high magnification micrographs (lower panel). **B)** CD45+ leukocytes within the perivascular cuffs in D16 EAE cerebellum as well as GFAP+ astrocytes that abut the perivascular cuffs express MCT-1, another lactate transporter. n=3 mice per group; scale bar – 50 μm.

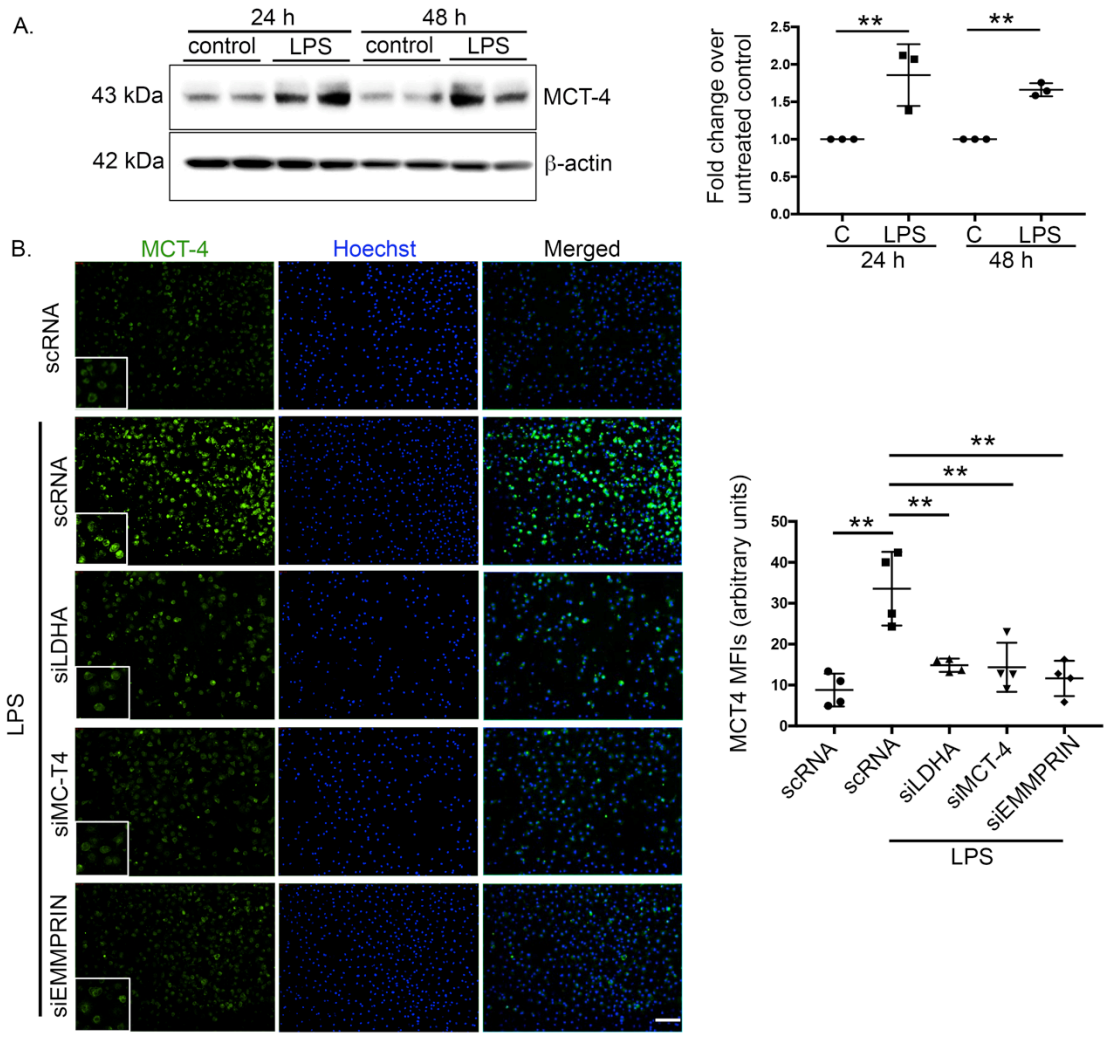

Figure S6. LPS-induced MCT-4 expression is regulated by LDHA and EMMPRIN. **A)** Immunoblot showing significant increase in MCT-4 levels upon 24 and 48h of LPS stimulation (100 ng/ml). **B)** Representative immunofluorescence images of MCT-4 (FITC, green) and nuclei (Hoechst) in different treatment conditions showing a decrease in membrane MCT-4 expression in LDHA and EMMPRIN-knockdown LPS-stimulated BMDMs along with MCT-4 knockdown, the positive control. The quantification is represented as MFIs of MCT-4 expression (right panel). Representative of 2 independent experiments run in quadruplicates; graphs are represented as mean±SD; Means were compared using one-way ANOVA with Tukey's post hoc test. **p<0.01. scale bar – 100 μm

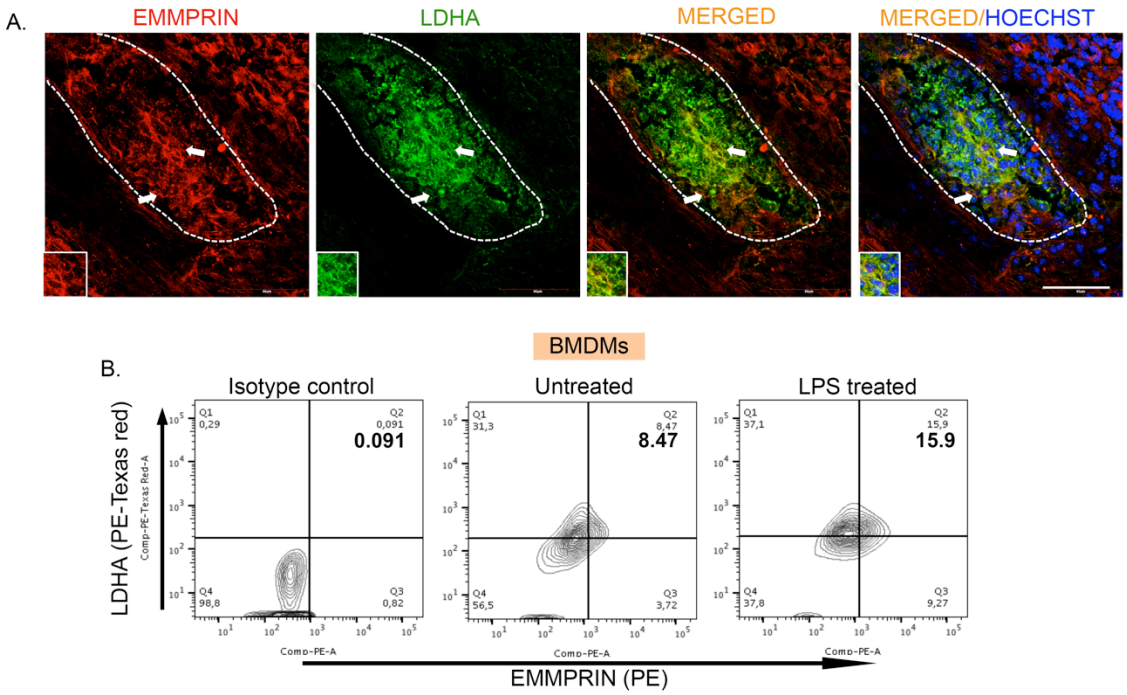

Figure S7. EMMPRIN is expressed in LDHA+ cells. A) Many cells within and around a perivascular cuff express EMMPRIN (red) and LDHA (green) in D16 EAE mice. Insets show magnified fields to highlight overlapping stains; scale bar – 50 μm. **B)** Flow cytometry analysis showing an increase in LDHA+ EMMPRIN+ cells upon 24 h of LPS stimulation in cultured BMDMs run in triplicate and representative of 2 independent experiments.

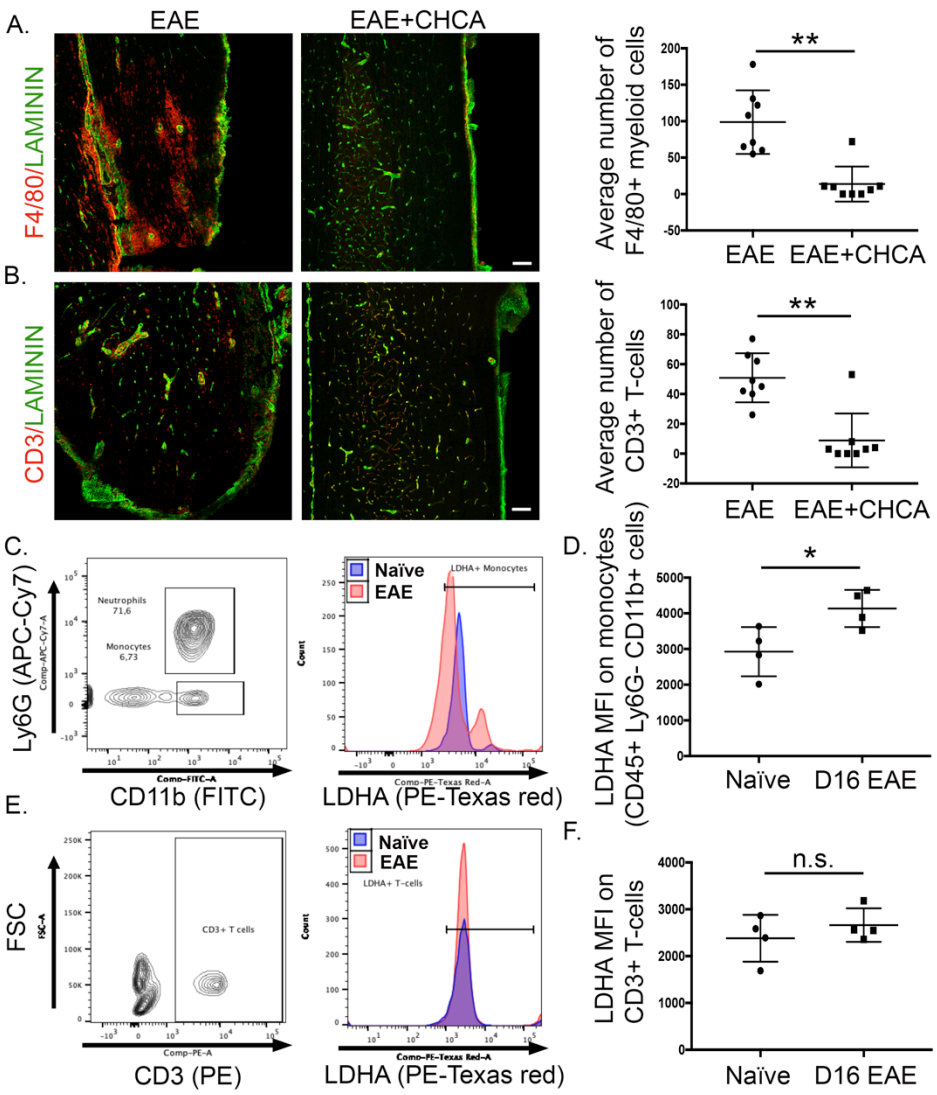

Figure S8. Effects of CHCA on T-cell migration in EAE and glycolytic profile of monocytes and T-cells during peak EAE. A) Confocal images (left panel) and graph (right panel) showing staining and quantification, respectively, of F4/80+ myeloid cells in EAE mice treated with vehicle or CHCA. **B)** Confocal images (left panel) and graph (right panel) showing staining and quantification, respectively, of CD3+ T-cells in EAE mice treated with vehicle or CHCA. 2 perivascular cuffs analyzed from 4 EAE mice; scale bar – 50 μm. **C)** Flow data plots showing gating strategies for monocytes (left panel) and LDHA expression in monocytes (right panel) in blood at peak EAE. **D)** Graph representing the LDHA MFI in monocytes in blood during peak disease severity as compared with naïve group. **E)** Gating strategy for CD3+ T cell population (left panel) and LDHA expression histograms (right panel) in CD3+ T cells in blood during peak EAE. **F)** Graph representing LDHA MFI in CD3+ T cells during peak disease severity as compared with naïve group. N=4 mice per condition analyzed. Graphs represented as mean±SD. Means were compared using two-tailed Student's t-test.*p<0.05, **p<0.01.

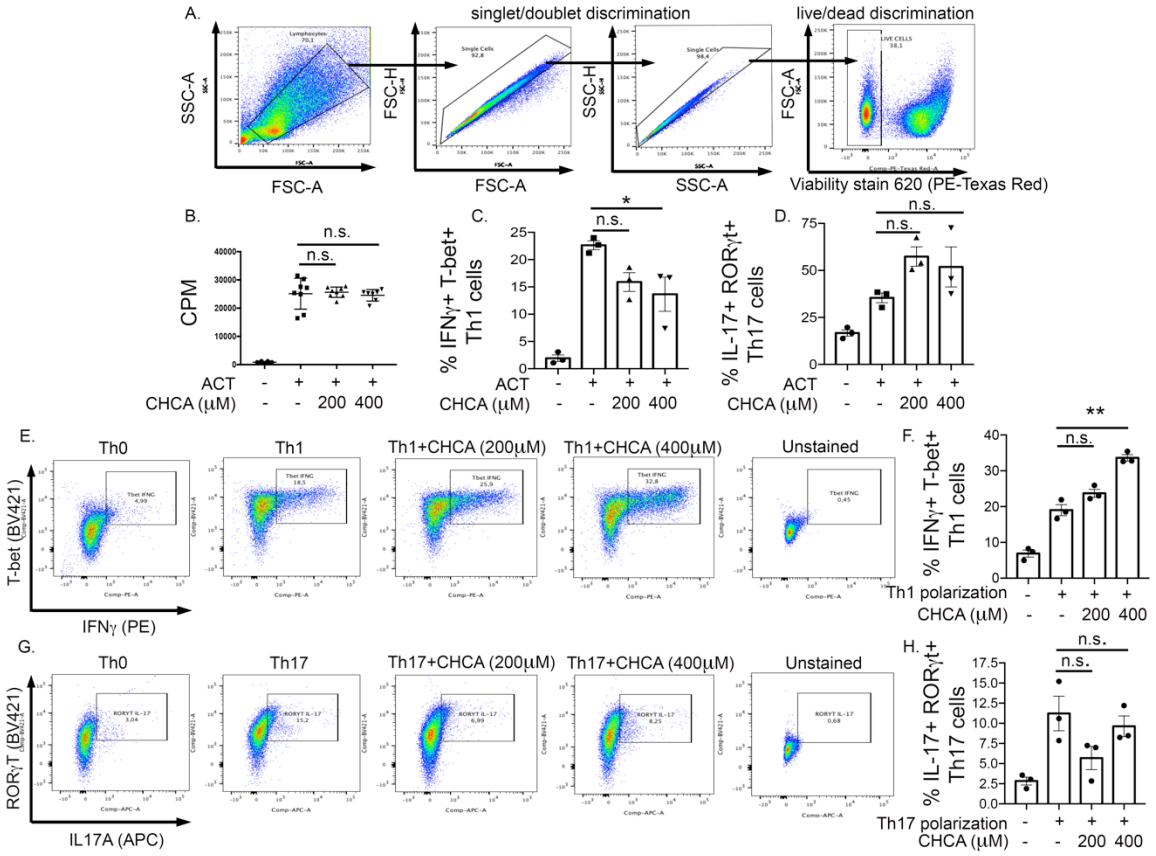

Figure S9. CHCA treatment alters T-cell polarization differently in splenocytes and pure T-cell cultures. A) Gating strategy on splenocytes for selection of single cells and live/dead discrimination. **B-D)** Graphs showing **B)** splenocyte proliferation measured as counts per minute (CPM), **C)** percentage of 'Th1-like' cells, and **D)** percentage of 'Th17-like' cells in presence of CHCA in polyclonally activated splenocytes. **E-H)** Polarization of pure T-cell cultures either into IFNγ+ T-bet+ Th1 **(E-F)** or IL-17+ RORγt+ Th17 **(G-H)** subsets in presence or absence of CHCA. 'No polarizing' condition represents Th0 polarization (a cocktail of IL-2 and anti-IFNγ and anti-IL-4 antibodies), Th1 polarizing cytokines is a cocktail of IL-2, IL-12 and anti-IL-4 antibody; Th17 polarizing cytokines is a cocktail of IL-6, TGF-β, IL-23 and anti-IFNγ and anti-IL-4 antibodies. Graphs representative of 2 independent experiments run in triplicate and represented as mean±SD. Means were compared using one-way ANOVA with Tukey's post hoc test. *p<0.05, **p<0.01.

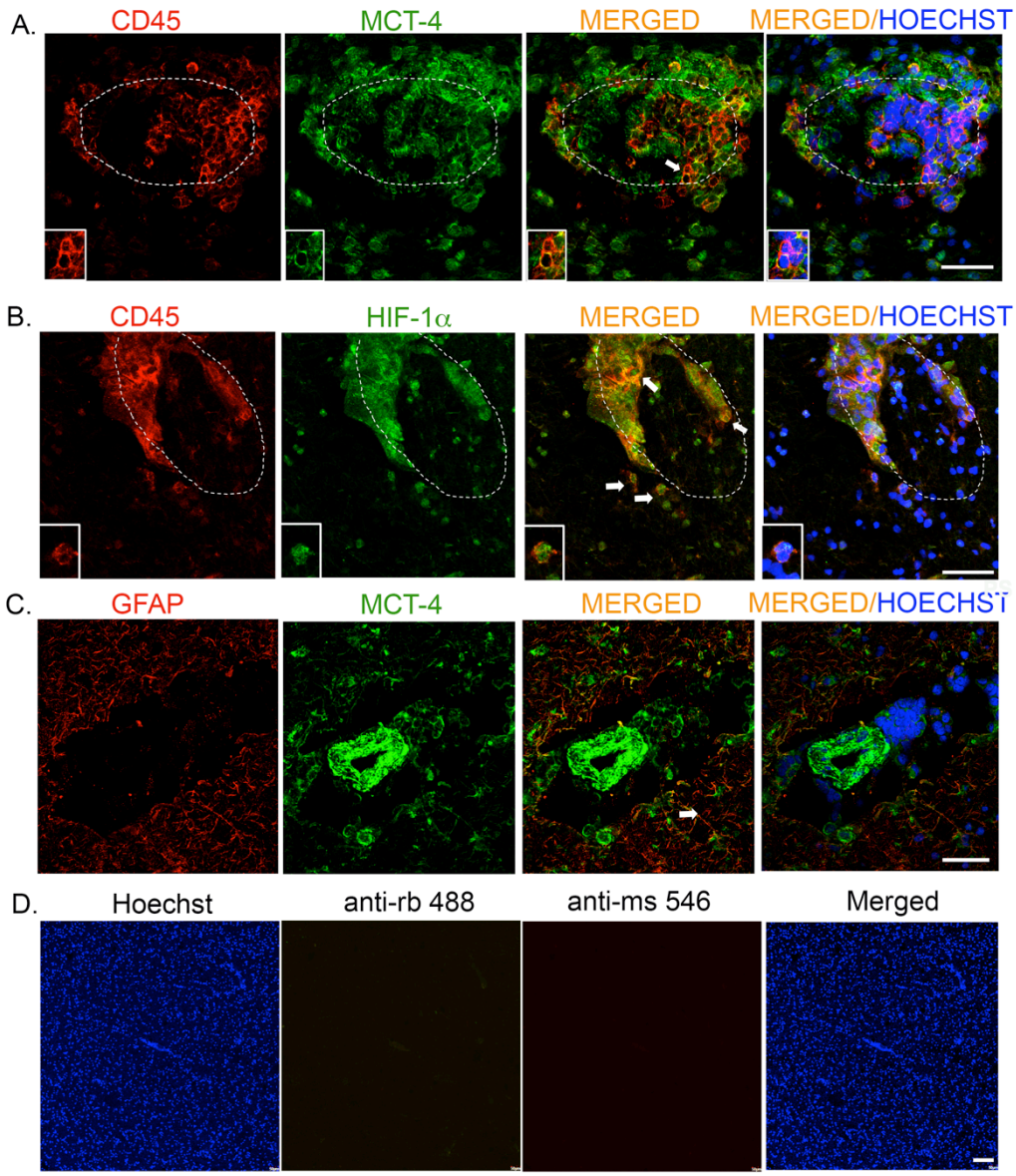

Figure S10. Expression of MCT-4, and HIF-1α in active brain lesions in MS. A-C) CD45+ leukocytes showing the expression of **A)** MCT-4, and **B**) HIF-1α in the inflamed cuffs within chronic MS brain lesions; insets show magnified cells. **C)** MCT-4 is also expressed on GFAP+ reactive astrocytes within the MS brain lesions; Representative of 3 different MS brains, two different active lesions per MS brain analyzed; scale bar – 50 µm. D) Images showing the 'secondary antibody only' controls using the anti-rb (anti-rabbit) 488, anti-mouse (anti-ms) 546 for MS brain sections, along with Hoechst staining the nuclei. Scale bar- 100 µm.

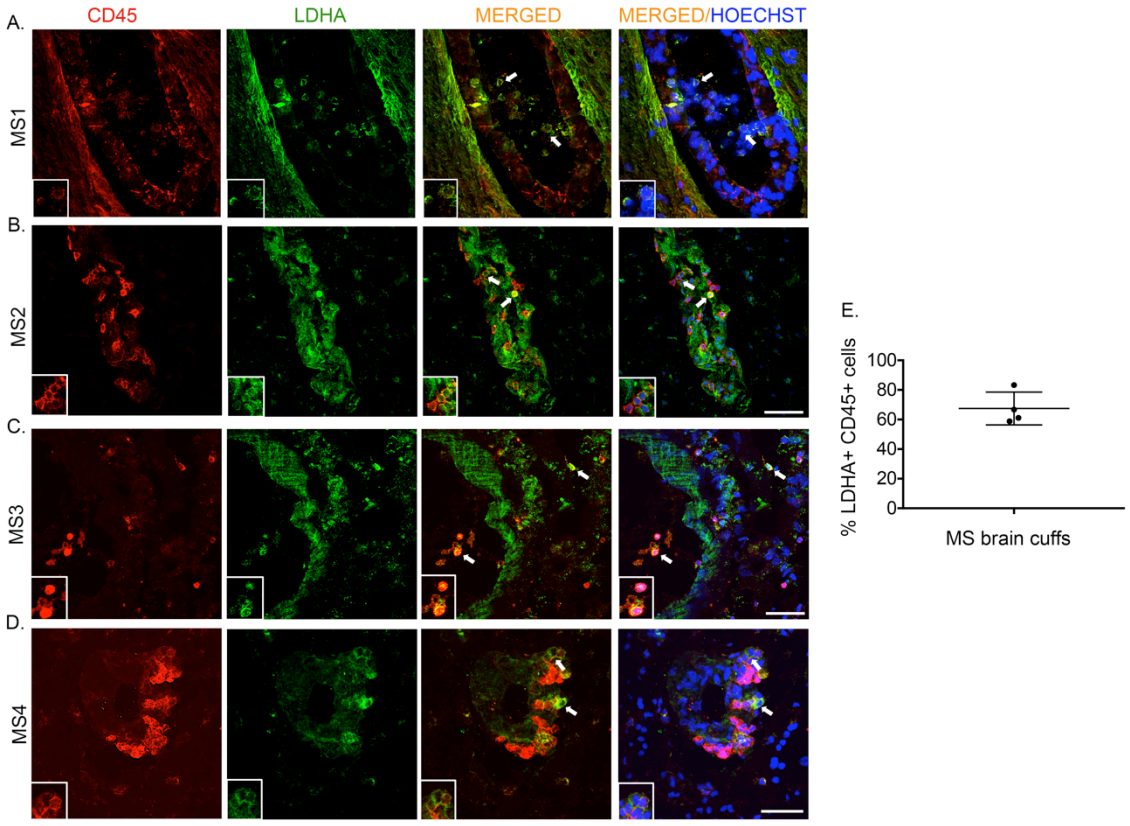

Figure S11. Glycolytic profile of 4 different MS brains. A-D) LDHA expression in CD45+ cells in the active lesions of **A)** MS1 (39y, F), **B)** MS2 (43y, M), **C)** MS3 (58y, F), and **D)** MS4 (82 y, F) brains. Representative images of two different active lesions per MS brain analyzed; Arrows indicate LDHA+ leukocytes and the insets show magnified cells; scale bar – 50 μm. **E)** Graph representing % LDHA+ CD45+ cells across these MS brains.